LBL-12173

CONF-811012--28

Lawrence Berkeley Laboratory
UNIVERSITY OF CALIFORNIA

Engineering & Technical Services Division

Presented at the 1981 IEEE Nuclear Science Symposium, San Francisco, CA, October 21-23, 1981, and to be published in IEEE Transactions on Nuclear Science, NS-29, No. 1 (1982)

A 300-MHz OPTICAL DISCRIMINATOR-COUNTER

B. Turko and C.C. Lo

July 1981

Prepared for the U.S. Department of Energy under Contract W-7405-ENG-48

A 300-MHz OPTICAL DISCRIMINATOR-COUNTER

B. Turko and C.C. Lo
Lawrence Berkeley Laboratory
University of California
Berkeley, California 94720

Abstract

The prediction of future CO_2 content in the atmosphere is not completely credible because the oceanographers and terrestrial ecologists do not agree on the global CO_2 balance. Very precise measurements of O_2/N_2 ratio using Raman scattering over a few years' period could provide important information and lead to the explanation of the disparity in the atmospheric CO_2 balance. An optical discriminator-counter has been developed to count closely spaced optical events in the few photon level. Simulated optical events as close as 2.5 ns apart had been positively detected by using selected photomultipliers and optimized discriminators. Testing of the optical discriminator-counter was done by using an electrical pulse pair spaced 3 ns apart and also by a similar optical pulse pair generated by fast light-emitting diode. The photomultiplier is capable of counting an average single photoelectron pulse frequency of 50 MHz and has a sensitive detecting area of 50 mm in diameter. The discriminator performance will be discussed.

Introduction

Global activities in the combustion of fossil fuels produce more and more carbon dioxide (CO_2) in the atmosphere. The ever increasing concentration of CO_2 may create the infamous greenhouse effect and cause catastrophic weather changes, leading to disastrous economic and social problems.

The prediction of future CO_2 content in the atmosphere is not completely credible because the oceanographers and terrestrial ecologists do not agree on the global CO_2 balance, (1). While there is no disagreement on the ever increasing CO_2 in the global atmosphere, very precise measurements of O_2/N_2 ratio over a few years' period could provide important information and lead to the explanation of the disparity in the atmospheric CO_2 balance.

Such experiments employing Raman scattering to determine O_2/N_2 molecular ratio have created the need for an optical counter able to detect single photon events with the best possible resolution and an average pulse counting capability of 50 MHz and which has, at the same time, a sensitive detecting area approximately 50 mm in diameter. A search of available detectors with single photon detection capability and all the aforementioned characteristics points to the RCA photomultiplier type C31024, (2). This five-stage RCA photomultiplier has a single photoelectron pulse width at half maximum of not more than 2 ns, making it possible for this device to detect events spaced approximately 3 ns apart. The single photoelectron pulses of this photomultiplier, however, having amplitude of only a few millivolt, require some amplification before they can be used to reliably, and positively, trigger a fast tunnel diode discriminator. To make the output of the discriminator acceptable to lower frequency scalers, a divide-by-four counter was incorporated into the discriminator so that the output pulse width could be stretched to 10 ns to meet the input requirement of a typical 100 MHz scaler.

The optical discriminator-counter was tested with electrical pulse pairs spaced 2.5 ns to 3 ns apart and also with similarly spaced optical pulse pairs generated by fast, light-emitting diode.

Electrical and Optical Test Pulses

Since the optical discriminator-counter is intended to be used to detect optical pulses as close together as 3 ns, electrical and optical pulses in this time range were generated for testing. Fig. 1 shows the system block diagram of our pulse generator.

A pulse generator, HP 215A, provided a fast pulse, having a FWHM width of 1.2 ns. A power divider split this pulse into two parts. One part was fed directly into one leg of a power combiner and the other was delayed by 3 ns with a delay cable before going to the other leg of the power combiner. The output pulse amplitude of the pulse from the combiner could be varied by an attenuator which followed it. The electrical pulse pair at this point was used in the development of the discriminator-counter. Fig. 2 shows a typical electrical pulse pair generated by this system.

To obtain an optical pulse pair the electrical pulses were amplified by a 10W linear amplifier having a bandwidth of 500 MHz. The output pulses of the amplifier were then used to drive a light-emitting diode, type XP-21, which operated in the avalanche mode. The XP-21 diode required a minimum drive in excess of 9V. The actual operating electrical pulses ranged from 15V - 22V for a 10% yield of single photoelectron pulses, as detected by the C31024 and C31024A photomultipliers.

The Photomultiplier Detector

The single photoelectron pulse response of the photomultiplier determined the pulse pair resolution of the system. Although there are other types of photomultipliers, (3,4,8,9), which can provide pulse widths less than the typical 1.5 ns of the RCA C31024A, they can neither provide the high counting rate required nor the large photocathode area offered by this device. The C31024A is a variant of the RCA C31024 and has five GaP dynodes. The C31024A has an RCA type 52AT ERMA II photocathode, which has a red response extending beyond 800 µm. The quantum efficiency of six C31024A's at 540 µm ranges from 8% to 11%. The average dark pulse count of four C31024A's ranges from 306 per sec. to 2880 per sec., summing from 1/8 photoelectron to 16 photoelectrons at room temperature. The single photoelectron pulse height ranges from 4mV - 15mV at the output of the photomultipliers terminated into a 50 ohm load. Fig. 2 shows a pair of typical single photoelectron pulses from a C31024A.

The maximum average anode current of the C31024A given by RCA is 100 µA; however, for long-term, stable operation, (5), only a fraction of this anode current should be used. Under 50 MHz single photoelectron pulse counting, the average anode current of the C31024A could reach 15 µA. Since photomultiplier fatigue varies widely even among tubes of the same type, monitoring the outputs from time to time may be necessary to ensure that the measurements are under control.

Fast Discriminator-Counter

Fig. 3 shows a schematic diagram of the discriminator-counter. A fast, 10 mA peak current tunnel diode is used as discriminator and is capable of resolving pulse pairs less than 3 ns apart, (6,7). The diode bias current is adjustable, (R14), to fire at the thresholds from 3mV to about 60mV (referred to in the input of the MITEQ, Inc. Model AV-2A-0550 wide-band amplifier). The tunnel diode load-line (resistor R11 and inductors L4 and L5) is adjusted to shape the output pulses so that they will be about 1.5 ns wide at each firing. The small input resistance at the tunnel diode in low level state in series with R10 provides a proper amplifier termination of 50 ohms. Correct termination and short ground loops are essential for stable, oscillation-free operation of the amplifier. For a short period after the diode firing the load is temporarily increased, and some charge is fed back to the output circuit of the amplifier. No instabilities due to this have been observed. Clamping diodes (CR 1 and CR 2) protect tunnel diode from transient damage during power turn-on. The amplifier output is capacitive-coupled. Only a small fraction of the transient current charging this capacitor to the power voltage passes through the tunnel diode, the major part being shunted by the diodes.

The tunnel diode negative output signal may vary significantly, especially when triggered by the tip of a small input pulse. The signal is increased and inverted in a wideband amplifier, (Q1). Also, the amplifier shifts the baseline of the signal to an appropriate negative level, providing the bias for the 350 MHz ECL counter stage (Motorola MC 1670). Optimum bias is obtained by adjusting R16. The counter is used only as divide-by-two stage without any provision for read-out or clear. Next, one half of the 250 MHz ECL counter (MC 10231) provides one more divide-by-two counter stage. The positive transition of the Q output of this stage takes place each time after a total of four tunnel diode transitions, resetting the last binary position of the counter. A feedback from the $\bar{Q}$ output to the set input, going positive, sets the binary to its original state after a delay defined by a capacitor. The binary performs as a monostable multivibrator, producing a shaped, 10 ns wide negative pulse at the Q output. The output current switching pair provides a standard NIM signal of 0.8V and 10 ns on a termination load resistance of 50 ohms.

Performance

The operating input signal level of the discriminator was measured by using an electrical pulse pair spaced 3 ns apart. The individual pulse width was 1.2 ns, measured at FWHM. The amplitude of the pulse pair was varied to find the minimum and maximum pulse height through which the discriminators operate properly. By using a pulse pair frequency of 1 MHz (2×10^6 pulses per second), the proper output pulse frequency of the discriminator is 5×10^5.

The ability of time-over-threshold discriminator to resolve two pulses 3 ns apart depends on their shape and on the relation of the amplitude to threshold setting. Two sets of double pulses were synthesized, simulating typical outputs of fast photomultipliers (Figs. 4 and 5). The pulses in Fig. 4 are narrower, which allows the valley between them to be set to zero. The pulses in Fig. 5 are wider, and their superposition lifts the valley off the baseline. The discriminator threshold setting and the shape of the pulses did not change as the amplitude was varied in order to determine limits of stable operation. The case of Fig. 4 is illustrated in Fig. 6 for two different amplitudes. The discriminator fires each time the leading edge of a pulse crosses the threshold. The recovery is slightly delayed due to hysterisis. The time between the recovery from the first pulse and the firing of the second ($t_2 - t_1$) grows smaller as the input pulse amplitudes are increased. At some point the recovery time is too short for the resolving capability of the circuits that follow the discriminator. At the lower amplitude end, however, the pulses that barely cross the threshold produce enough discriminator output to advance the counter. Proper threshold selection is thus important to obtain an optimum input amplitude dynamic range. Reducing the threshold may not increase the ratio between the highest and lowest accepted signals, since the recovery time, t_2, would be decreased. An optimum must be found for each individual photomultiplier-discriminator set.

The case of Fig. 5 is illustrated in Fig. 7. The two pulses will be resolved as long as the valley stays under the threshold level for a sufficient time, t_1. The valley between a higher pulse pair never returns to below the threshold and the pair is interpreted by the discriminator as a single event. Measurements were made on three discriminators for their trigger levels as a function of ambient operating temperature. The results are given in Fig. 8.

Conclusions

The large-area optical discriminator-counter described was capable of detecting single photoelectron events spaced as closely as 2.5 ns apart by using selected photomultipliers, tunnel diodes and other key components.

The preamplifier at the input of the discriminator-counter has a bandwidth of 500 MHz and a noise figure of not higher than 2 dB. Optical detectors such as microchannel plate photomultipliers have much better pulse pair resolution capabilities, but they lack the ability of high frequency counting, which is usually limited between 0.1 - 1 MHz at single photon level.

Acknowledgement

The work was performed as part of the program of the Electronics Research and Development Group of the Lawrence Berkeley Laboratory, Berkeley, California, and was supported by the Department of Energy under Contract No. W-7405-ENG-48 and the National Oceanic and Atmospheric Administration.

References

1. P.P. Tans et al., *Determination of the Atmospheric* Carbon Dioxide Budget by Precise Measurements of the Oxygen to Nitrogen Molecular Ratio, Research Proposal, Lawrence Berkeley Laboratory, 1980.

2. C.C. Lo, Branko Leskovar, A Measuring System for Studying the Time-Resolution Capabilities of Fast Photomultipliers, IEEE Trans. Nucl. Sci., NS-21, No. 1, February, 1974, pp. 93-105.

3. C.C. Lo, Branko Leskovar, Studies of Prototype High-Gain Microchannel Plate Photomultipliers, IEEE Trans. Nucl. Sci., NS-26, No. 1, February, 1979, pp. 388-394.

4. Branko Leskovar, C.C. Lo, Time-Resolution Performance Studies of Contemporary High-Speed Photomultipliers, IEEE Trans. Nucl. Sci., NS-25, No. 1, February, 1978, pp. 582-586.

5. C.C. Lo, Branko Leskovar, Performance Studies of the New Generation Amperex XP2020 Photomultiplier, IEEE Trans. Nucl. Sci., NS-28, No. 1, February, 1981, pp. 659-665.

6. Bojan Turko, Space-Borne Event Timer, IEEE Trans. Nucl. Sci., NS-27, No. 1, February, 1980, pp. 399-404.

7. Bojan Turko, A Picosecond Resolution Time Digitizer for Laser Ranging, IEEE Trans. Nucl. Sci., NS-25, No. 1, February, 1978, pp. 75-80.

8. J.P. Boutot, The HR 400, Microchannel Plate Photomultiplier with a High Gain and Low Noise, (in French), Rapport de la 4e Journee d'Optique Spatiale, Marseille, France, November, 1973, pp. 291-300.

9. C.C. Lo, Branko Leskovar, Performance Studies of High Gain Photomultiplier Having Z-Configuration of Microchannel Plates, IEEE Trans. Nucl. Sci., NS-28, No. 1, February, 1981, pp. 698-704.

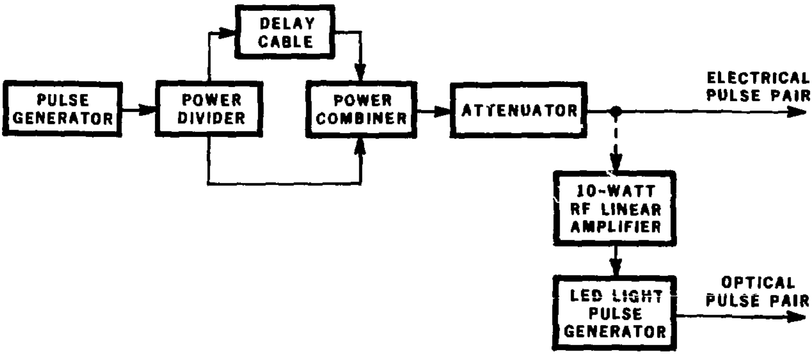

XBL 814-9261

Fig. 1 Block diagram of the electrical and optical pulse pair generation system

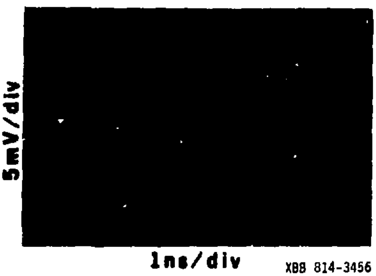

XBB 814-3456

Fig. 2 Photomultiplier C31024A single photoelectron output pulses

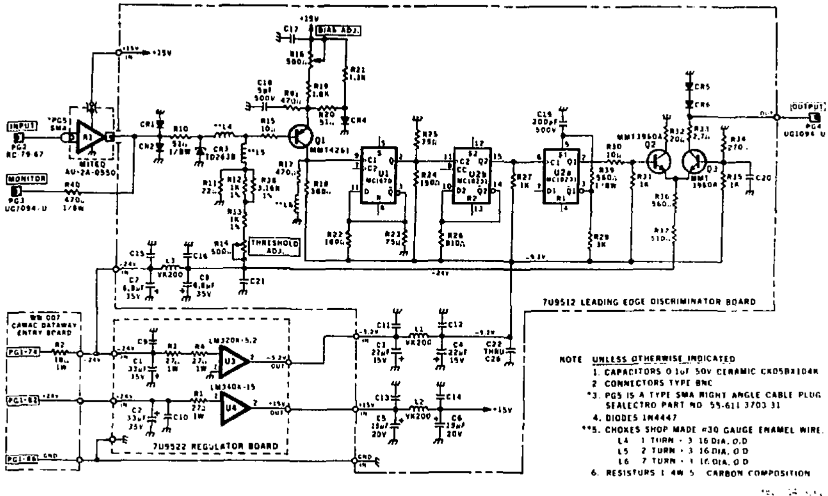

Fig. 3 Discriminator-counter circuit diagram

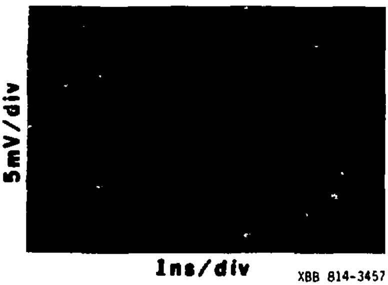

Fig. 4 Electrical pulse pair with 1.2 ns pulse width at FWHM

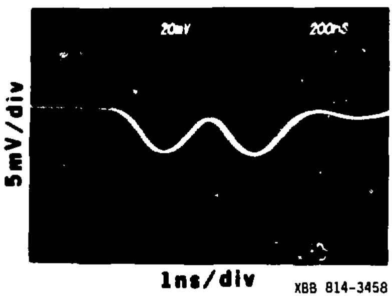

Fig. 5 Electrical pulse pair with 2 ns pulse width at FWHM

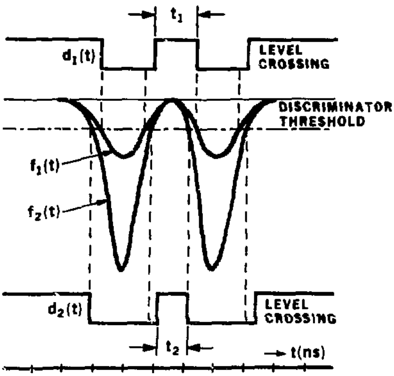

XBL 814-9264

Fig. 6 Discriminator triggering thresholds with the 1.2 ns pulse pair

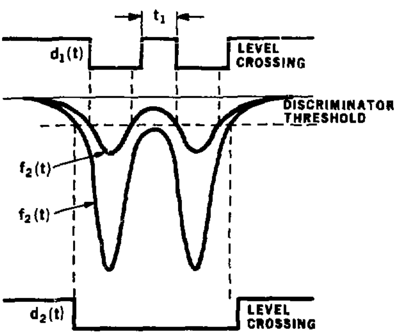

XBL 814-9263

Fig. 7 Discriminator triggering thresholds with the 2 ns pulse pair

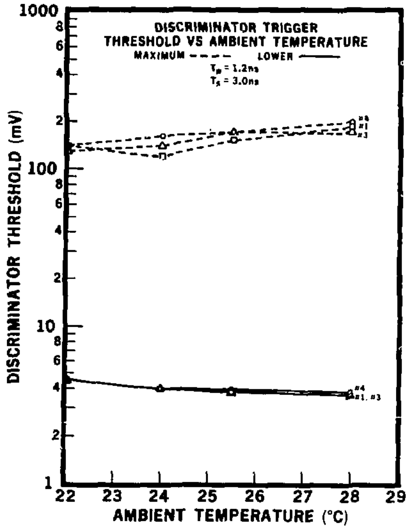

Fig. 8 Discriminator-counter trigger threshold as a function of ambient temperature